Journal of Field Robotics

WILEY

RESEARCH ARTICLE OPEN ACCESS

Collaborative Sampling and Imaging of Phytoplankton Communities by Two Long-Range Autonomous Underwater Vehicles Using Acoustic Tracking and Messaging

Yanwu Zhang | Brian Kieft | Monique Messié | Quinn Shemet | Brett W. Hobson | Paul Roberts | Brent Jones | Michael Anderson | Thom Maughan | Varsha Senthil

Monterey Bay Aquarium Research Institute, Moss Landing, California, USA

Correspondence: Yanwu Zhang (yzhang@mbari.org)

Received: 26 November 2024 | **Revised:** 28 June 2025 | **Accepted:** 10 November 2025

Funding: This study was supported by the David and Lucile Packard Foundation.

Keywords: autonomous robot | field robotics | multi-robot cooperation

ABSTRACT

Collaborative operation of multiple autonomous underwater vehicles (AUVs) can effectively achieve scientific goals that are hard to achieve by independently operated vehicles. Some science payloads are large, expensive, and need to be installed in the vehicle's nose cone. A vehicle can only carry one such payload. This specialization leads to heterogeneous fleets of vehicles that must work collaboratively to investigate unique oceanographic features using complementary payloads. We present a method of using acoustic tracking and messaging between two long-range AUVs (LRAUVs) with different payloads for collaborative sampling and imaging of phytoplankton communities. The sampling vehicle acquires water samples from the peak chlorophyll layer. The imaging vehicle acoustically tracks the sampling vehicle and takes microscopic images of the surrounding water column to provide contextual optical evidence. Each vehicle transmits acoustic messages to inform the other vehicle about distance or mission status. In this collaboration, acoustic tracking and messaging enable co-located synchronized sampling and imaging. The method was used in phytoplankton studies in Monterey Bay, California, in August 2024.

1 | Introduction

Coordinated operation of a team of robots has the potential of accomplishing tasks more effectively than independently operated vehicles, such as in aerial search and rescue missions (Skorobogatov et al. 2020), subterranean exploration (O'Brien et al. 2023), and fish tracking (Lin et al. 2017). Navigation and coordination of multiple autonomous underwater vehicles (AUVs) were explored in simulations (Paull et al. 2015; Yilmaz et al. 2008) and field experiments (Lin et al. 2017; Fischell et al. 2019; Rypkema et al. 2022).

Teams of AUVs under coordinated control or using inter-vehicle tracking were deployed in scientific expeditions. For estimating heat flux at a coastal upwelling center to the north of Monterey Bay, California, a coordinated fleet of underwater gliders patrolled along the boundary of a control volume (Leonard et al. 2010; Paley et al. 2008). The commands from the onshore control system were transmitted via the Iridium satellite to the gliders when the gliders periodically ascended to the surface. Two AUVs were deployed for studying internal waves in the Tyrrhenian Sea (Petillo and Schmidt 2014). One AUV with relatively high navigation precision ran on a pentagonal track and the second AUV acoustically trailed the first AUV while measuring temperature and salinity within the thermocline. In a Hawaiian eddy, a system of three autonomous vehicles conducted a Lagrangian study of the microbial community in the deep chlorophyll maximum (DCM) layer (Zhang et al. 2021). A *Tethys*-class long-range AUV (LRAUV) was equipped with a Third-Generation Environmental Sample Processor (3G-ESP), a robotic instrument for acquiring and processing water samples for molecular analysis (Scholin et al. 2017). Over 4 days, the sampling LRAUV continuously tracked the DCM layer and acquired water samples at 3-h intervals. A second LRAUV acoustically tracked the sampling LRAUV and spiraled up and down around it to make contextual measurement. A Wave Glider (Hine et al. 2009; Manley and Willcox 2010) at the surface also autonomously tracked the sampling LRAUV to provide situational awareness.

Exchange of key information between AUVs enables the vehicles to promptly adapt behaviors and accomplish tasks efficiently. In a multi-AUV fish tracking experiment (Lin et al. 2017), the fish was tagged with an acoustic transmitter. Each AUV carried a two-hydrophone array and an acoustic modem. Each "follower AUV" transmitted the distance-to-tag and bearing-to-tag estimates to the "leader AUV." The AUVs coordinated to circumnavigate the fish at the desired radius and even spacings. In a lake experiment for locating an isobath (Biggs et al. 2024), a team of AUVs exchanged acoustic messages containing path and depth measurements to jointly optimize the search path. In Monterey Bay, we deployed two LRAUVs (each equipped with a 3G-ESP) to achieve continuous and persistent environmental DNA (eDNA) sampling of vertically migrating organisms at a targeted depth layer (Zhang et al. 2024). When one vehicle was conducting ESP sampling at the targeted depth, the other vehicle was spiraling over a large depth range to make contextual measurement. We field-tested a collaborative sampling method based on acoustic messaging. When vehicle #1 completed a sampling event, it transmitted a sample-end message to vehicle #2. On receiving this message, vehicle #2 triggered a sampling event and transmitted a sample-start message to vehicle #1, and so forth. These acoustic handshakes realized a seamless passing of the sampling "baton."

To achieve the scientific goal of precisely characterizing the taxonomic composition of phytoplankton communities, we developed a method of using two LRAUVs (equipped with an eDNA sampler and a microscopy system, respectively) for co-located and synchronized sampling and imaging using inter-vehicle acoustic tracking and messaging. The sampling vehicle acquires water samples from the peak chlorophyll layer for subsequent molecular analysis in the shore lab after vehicle recovery. The imaging vehicle takes microscopic images of the surrounding water column to provide contextual optical evidence.

The *Tethys*-class LRAUV is introduced in Section 2. The collaborative sampling and imaging algorithms are presented in Section 3. Experiments in Monterey Bay in August 2024 are reported in Section 4. Conclusion and future work are discussed in Section 5.

2 | LRAUVs Equipped With DAT, Microscopy System, and Water Sampler

Tethys-class LRAUVs were developed at the Monterey Bay Aquarium Research Institute (MBARI). Each vehicle is 2.3 m long (in basic configuration) and has a diameter of 0.3 m at the midsection (Figure 1). It can run from 0.5 to 1.4 m/s using a propeller. Using a primary battery, the vehicle has demonstrated a range of 1800 km (3-week duration) at 1 m/s speed (Hobson et al. 2012). Long range is realized by minimizing propulsion power consumption through an innovative design of a low-drag body, a high-efficiency propulsion system, and selective load control (Bellingham et al. 2010; Hobson et al. 2012). In addition, the vehicle is equipped with a buoyancy engine and is capable of auto-ballasting to neutral buoyancy, which allows flight at a reduced angle of attack resulting in decreased drag. Using the buoyancy engine, the vehicle is capable of drifting in a

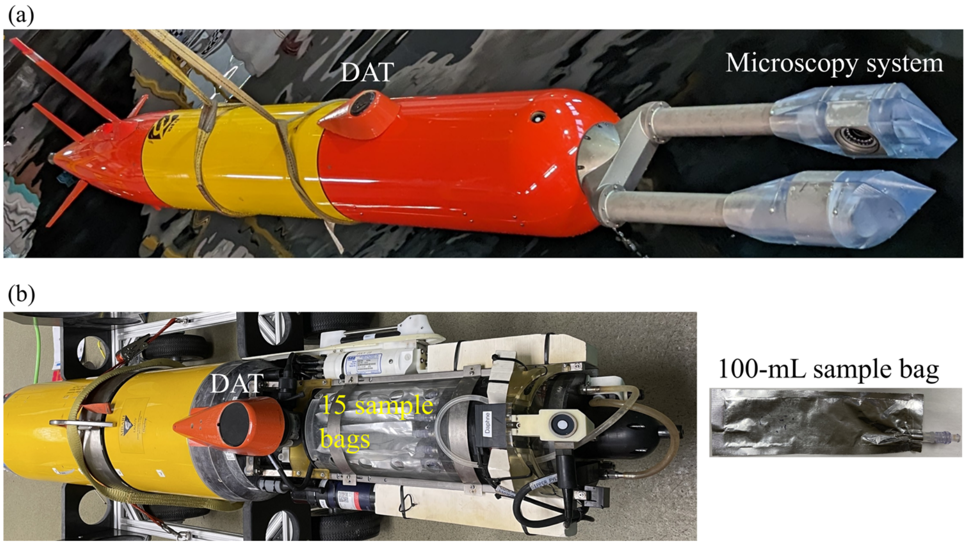

FIGURE 1 | A *Tethys*-class LRAUV equipped with a directional acoustic transponder (DAT) and a "Planktivore" microscopy system (a). Another LRAUV with a DAT and a "Sipper" water sampler containing 15 100-mL bags (b). [Color figure can be viewed at wileyonlinelibrary.com]

lower power state and controlling depth while the thruster is powered off. An LRAUV thus combines mobility and speed properties typical of propelled vehicles and the energy-saving properties unique to buoyancy-driven vehicles.

An LRAUV's standard science sensor suite includes Sea-Bird Glider Payload Conductivity-Temperature-Depth (GPCTD) sensors, a Sea-Bird SBE 43F dissolved oxygen sensor, a WET Labs ECO Triplet Puck fluorescence/backscatter sensor (chlorophyll fluorescence excitation wavelength 470 nm and emission wavelength 695 nm; backscatter of two wavelengths: 470 nm and 650 nm), and a LI-COR LI-192SA PAR (photosynthetically active radiation) sensor. The vehicle's underwater navigation is by dead reckoning aided by a Doppler Velocity Log (DVL). The DVL provides the Earth-referenced velocity of the vehicle when the ocean bottom is within acoustic range. The vehicle's estimated speed is combined with measured heading and attitude and then accumulated to provide the estimated location while underwater. The vehicle periodically ascends to the surface for global positioning system (GPS) fixes to correct the accumulated underwater navigation error (Hobson et al. 2012).

The LRAUV software architecture uses state configured layered control (Bellingham and Consi 1990), which divides the vehicle operation into a group of behaviors assigned with hierarchical levels of priority. The vehicle runs a mission script that invokes appropriate AUV behaviors to achieve a specified goal (Hobson et al. 2012).

A Teledyne Benthos directional acoustic transponder (DAT) (Figure 1) integrates an acoustic modem and an ultra-short baseline (USBL) acoustic positioning system (Stanway et al. 2014). Using the USBL system, the tracking vehicle estimates the range and direction of the tracked vehicle, and accordingly updates its own commanded position to follow the tracked vehicle at the desired standoff distance. Using the acoustic modem, messages can be acoustically transferred between LRAUVs as well as to surface vehicles. Currently, full command and control of the LRAUV are implemented over the acoustic layer which supports transmitting and ingesting mission variables. Acoustic messaging enables LRAUVs to work collaboratively based on real-time exchanges of sensor data and vehicle operation status while remaining underwater within the targeted oceanographic feature.

An in situ microscopy system (nicknamed "Planktivore", developed at MBARI) can be installed at the nose of the LRAUV (Figure 1). The design of "Planktivore" was based on the Scripps Plankton Camera System (Orenstein et al. 2020) but adapted to work on autonomous vehicles. It uses two complementary microscope objectives (each with a camera and a light-emitting diode (LED) strobe) focused on a free-space volume in water roughly 12 mm away from each of the two viewports. This configuration enables free-space imaging of plankton, marine snow, and other suspended material that enter the sample volume via ambient flow and helps to reduce avoidance. The pair of cameras (of high and low magnification respectively) cover a particle size range from 20 μm to 2 cm.

Alternatively, a water sampler (nicknamed "Sipper" (Chavez et al. 2017), developed at MBARI) can be installed inside the nose cone of the vehicle (Figure 1). It contains 15 Mylar polyethylene-lined bags each of 100-mL volume when filled. The 15 bags have one-way valves and are arranged in a carousel. Seawater is ingested through a peristaltic pump and plumbed directly into the bag, taking about 4 minutes to fill a bag. The carousel rotates to align each successive sampling bag with the pump outlet.

3 | Two-LRAUV Collaborative Sampling and Imaging of Phytoplankton Communities

The goal of the collaborative operation was to use a sampling LRAUV and an imaging LRAUV to simultaneously and efficiently acquire water samples in the peak chlorophyll layer and take microscopic images of the surrounding water column. In a previous experiment, we deployed two such LRAUVs to achieve this goal, but we did not use inter-vehicle acoustic messaging. The need for the operator's monitoring and manual commands adversely affected efficiency. First, both vehicles transited to the sampling waypoint. The shore operator monitored the two vehicles' locations (when each vehicle periodically surfaced for GPS fixes and Iridium satellite communications). As the two vehicles successively surfaced at the sampling waypoint, the shore operator sent "stop" commands and new missions individually to the imaging and sampling vehicles, all via the Iridium satellite. The operator needed to carefully time the sendings of the imaging and sampling missions: first to the imaging vehicle and then to the sampling vehicle to ensure the entire sampling duration was fully covered by imaging. When the sampling vehicle completed sampling and ascended to the surface, the shore operator sent a "stop" command to the imaging vehicle to terminate its mission (the "stop" command was to be received on the vehicle's next surfacing).

The above process required the operator to watch closely and intervene often. The operator needed to check the two vehicles' arrivals at the sampling waypoint and manually kick off the imaging and sampling missions, which introduced some delay. After the sampling vehicle had completed sampling, the imaging vehicle spent extra time underwater until the next surfacing when receiving the "stop" command. These drawbacks motivated us to utilize inter-vehicle acoustic messaging to enhance efficiency of the two vehicles' collaborative operation.

3.1 | Collaborative Sampling and Imaging Using Acoustic Tracking and Messaging

At each sampling waypoint, one LRAUV acquires water samples in the peak chlorophyll layer while another LRAUV simultaneously takes images of the surrounding water column. The steps of the collaborative operation are illustrated in Figure 2 and elaborated as follows. For brevity, henceforth the sampling and imaging LRAUVs are denoted by AUV_s and AUV_i, respectively.

- Both vehicles transit to the sampling waypoint on a sawtooth (i.e., yo-yo) trajectory in the vertical dimension. If AUV_s reaches the waypoint before AUV_i, it spirals up and down to wait for AUV_i (i.e., the "wait" phase). If AUV_i reaches the waypoint before acoustically detecting AUV_s, it spirals up and down and attempts to detect AUV_s using the

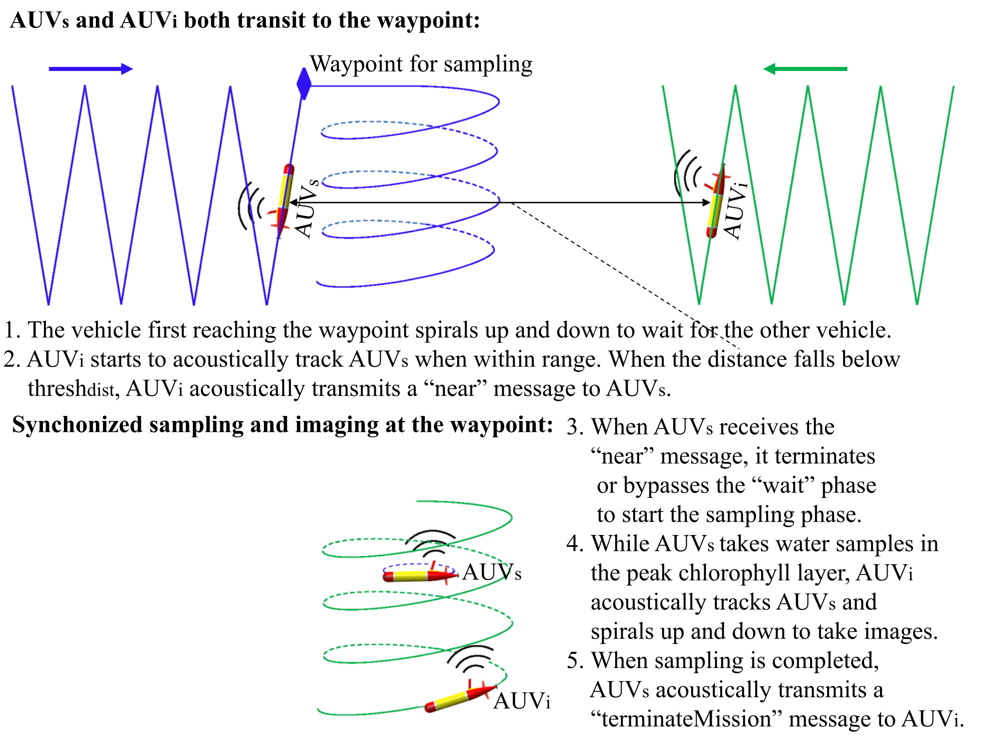

FIGURE 2 | Diagram of collaborative sampling and imaging by two LRAUVs. [Color figure can be viewed at wileyonlinelibrary.com]

DAT (with an acoustic range of about 2 km). On detection of AUV_s, AUV_i acoustically tracks AUV_s until AUV_s reaches the waypoint.

- When the distance between the two vehicles falls below a threshold $thresh_{dist}$, AUV_i acoustically transmits a "near" message to AUV_s.
- AUV_s receives the "near" message.
  - If AUV_s receives the "near" message before reaching the waypoint, it will continue the transit to the waypoint, and then bypass the "wait" phase to start the sampling phase.
  - If AUV_s has already entered the "wait" phase at the sampling waypoint and then receives the "near" message, it will exit the "wait" phase to start the sampling phase.
- In the sampling phase, AUV_s autonomously finds the peak chlorophyll layer (see Section 3.2) to acquire water samples in that layer. While AUV_s takes water samples, AUV_i spirals up and down around AUV_s to take microscopic images in the surrounding water column.
- When AUV_s has finished sampling, it acoustically transmits a "terminateMission" message to AUV_i. When AUV_i receives this message, it terminates the imaging mission. The joint operation ends.

3.2 | Autonomous Detection and Sampling of the Peak Chlorophyll Layer

In the sampling phase, AUV_s operates in the following steps to autonomously find the peak chlorophyll layer and acquire water samples in this layer (Zhang et al. 2020). The steps are illustrated in Figure 3, labeled with the corresponding step number.

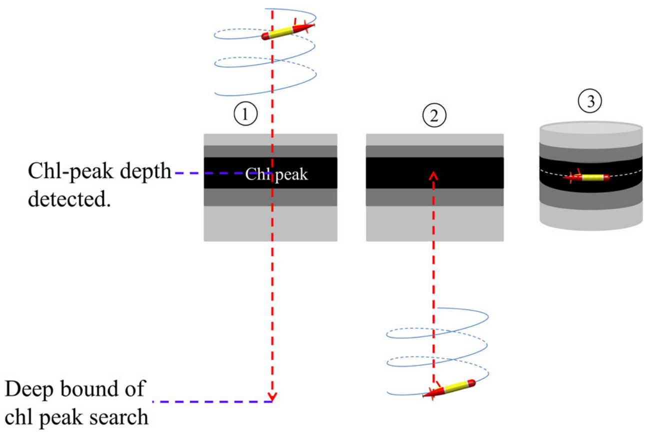

FIGURE 3 | Illustration of the algorithm for AUV_s to autonomously find the peak chlorophyll layer. The gray scale represents the chlorophyll signal level. The darkest layer represents the peak chlorophyll layer. [Color figure can be viewed at wileyonlinelibrary.com]

- AUV_s seeks the chlorophyll signal peak in the depth range from $Dep_{ShallowBoundChl}$ (water sampling should not happen shallower than this bound to prevent air intake) and $Dep_{DeepBoundChl}$ (this bound is sufficiently deeper than the anticipated peak chlorophyll depth). From the sea surface, the vehicle spirals down to $Dep_{DeepBoundChl}$.
- Upon reaching the depth $Dep_{DeepBoundChl}$, AUV_s turns to an upward spiral and records the peak chlorophyll signal value on the just-completed descent leg and the corresponding depth.
- On the ascent, when AUV_s reaches the peak chlorophyll depth, it stops ascending and circles at that depth to take water samples.

4 | Field Experiments

The scientific goal of the August 2024 experiments in Monterey Bay was to characterize the taxonomic composition of phytoplankton communities at five contrasting sampling sites using two different yet complementary techniques (eDNA sampling and in situ microscopy) to validate proxies (computed from LRAUV measurements) for distinct phytoplankton groups. For accurate comparison between the results of the two techniques and proxy validation (Messié et al. 2019), the eDNA sampling vehicle and the microscopic imaging vehicle needed to be co-located.

Two LRAUVs were deployed: AUV_s carried the "Sipper" water sampler and AUV_i carried the "Planktivore" microscopy system. We selected a sequence of sampling waypoints using preceding LRAUV survey data based on the following criteria: (1) comparatively high levels of chlorophyll which is associated with phytoplankton abundance (Falkowski and Kiefer 1985), (2) phytoplankton communities dominated by diatoms or dinoflagellates. Taxonomic information was obtained from onboard real-time processing of the microscopic images and also from an onboard machine-learning proxy trained on past data.

For example, Figure 4 shows a subset of the images taken by AUV_i's microscopy system during the August 29 experiment. The images capture the diversity of sizes and genera observed during AUV_s's sampling phase.

A total of five sampling waypoints were selected over the course of the deployment, with each sampling event triggering three bags to ensure a sufficient volume of water for subsequent eDNA analysis in the lab. Here, we describe two such sampling events. The parameter settings are listed in Table 1.

To define the depth range for finding the peak chlorophyll in AUV_s's sampling phase, $Dep_{ShallowBoundChl}$ and $Dep_{DeepBoundChl}$ were set to 2 and 20 m, respectively. For triggering the acoustic transmission of the "near" message (from AUV_i to AUV_s), the distance threshold $thresh_{dist}$ was set to 100 m. For the DAT's acoustic communications to operate reliably, the device should be submerged below a sufficient depth. The DAT is mounted on the upper side of the nose section of the LRAUV (Figure 1) while the depth sensor is installed in the tail section. Considering the distance between the two devices and the vehicle's pitch-up attitude on ascent, we set a minimum depth for enabling the operation of the DAT's modem: Dep_{minDAT}. When the vehicle's depth reading is shallower than Dep_{minDAT}, the DAT will not transmit acoustic messages. In the experiments, we set Dep_{minDAT} to 2 m.

After sending a message, the transmitting vehicle expects an acknowledgment from the receiving vehicle. If not getting the acknowledgment, the transmitting vehicle will re-send the message (called a "retry"). The maximum number of retries $Retries_{maxDAT}$ was set to four in the experiments.

4.1 | Experiment on August 28, 2024

The sampling waypoint was at 36.9026°N, 121.9636°W. The time series of AUV_s and AUV_i's depths (color coded by

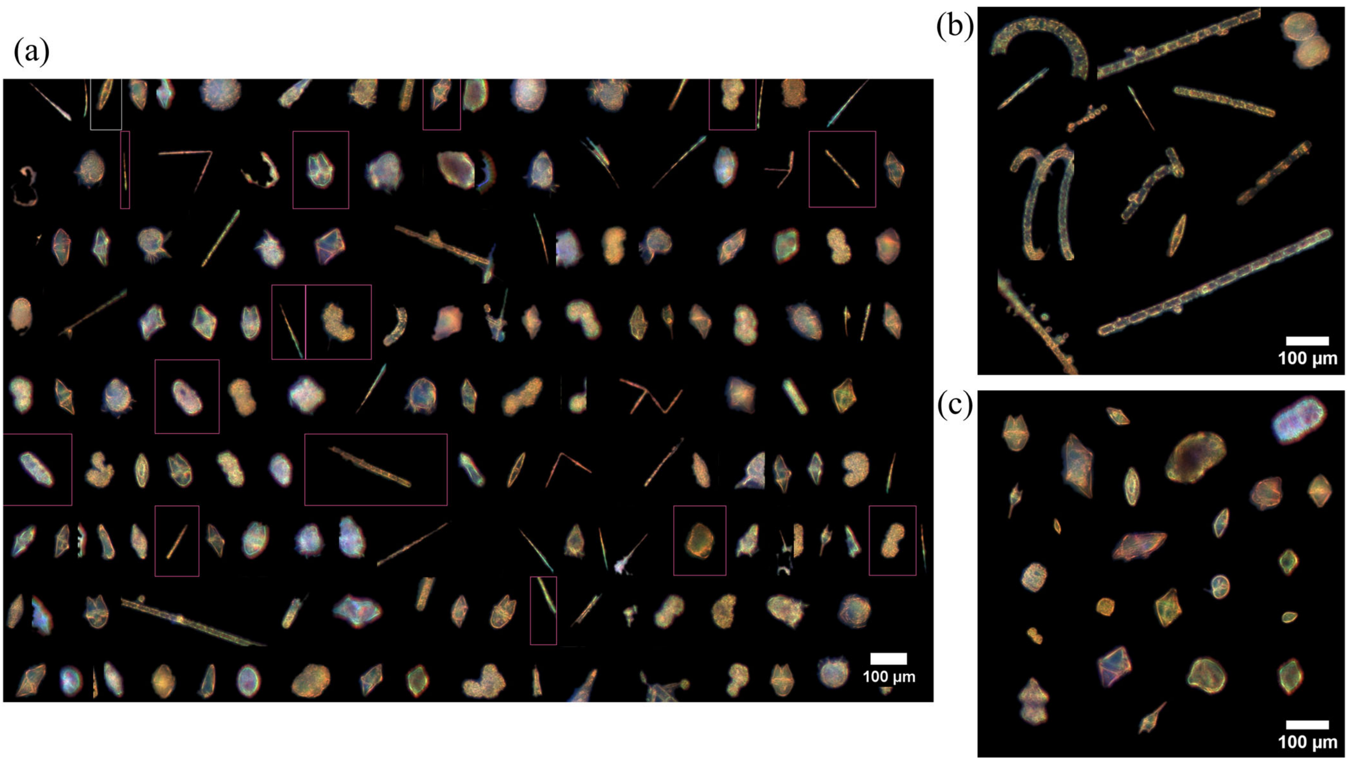

FIGURE 4 | Mosaic of a subset of phytoplankton images (5600 in total) automatically detected and recorded from the high-magnification camera from 15:40 to 16:10 (PDT) in the August 29 experiment (a). Selected images of diatoms (b) and dinoflagellates (c). [Color figure can be viewed at wileyonlinelibrary.com]

TABLE 1 | Parameter settings in the August 2024 experiments.

Parameter	Meaning	Setting
$Dep_{ShallowBoundChl}$	The shallow bound for finding the chlorophyll peak	2 m
$Dep_{DeepBoundChl}$	The deep bound for finding the chlorophyll peak	20 m
$thresh_{dist}$	When the distance to the other LRAUV ≤ $thresh_{dist}$, this vehicle transmits "near" message.	100 m
Dep_{minDAT}	The minimum depth for enabling DAT's modem	2 m
$Retries_{maxDAT}$	The maximum number of resendings of the message	4

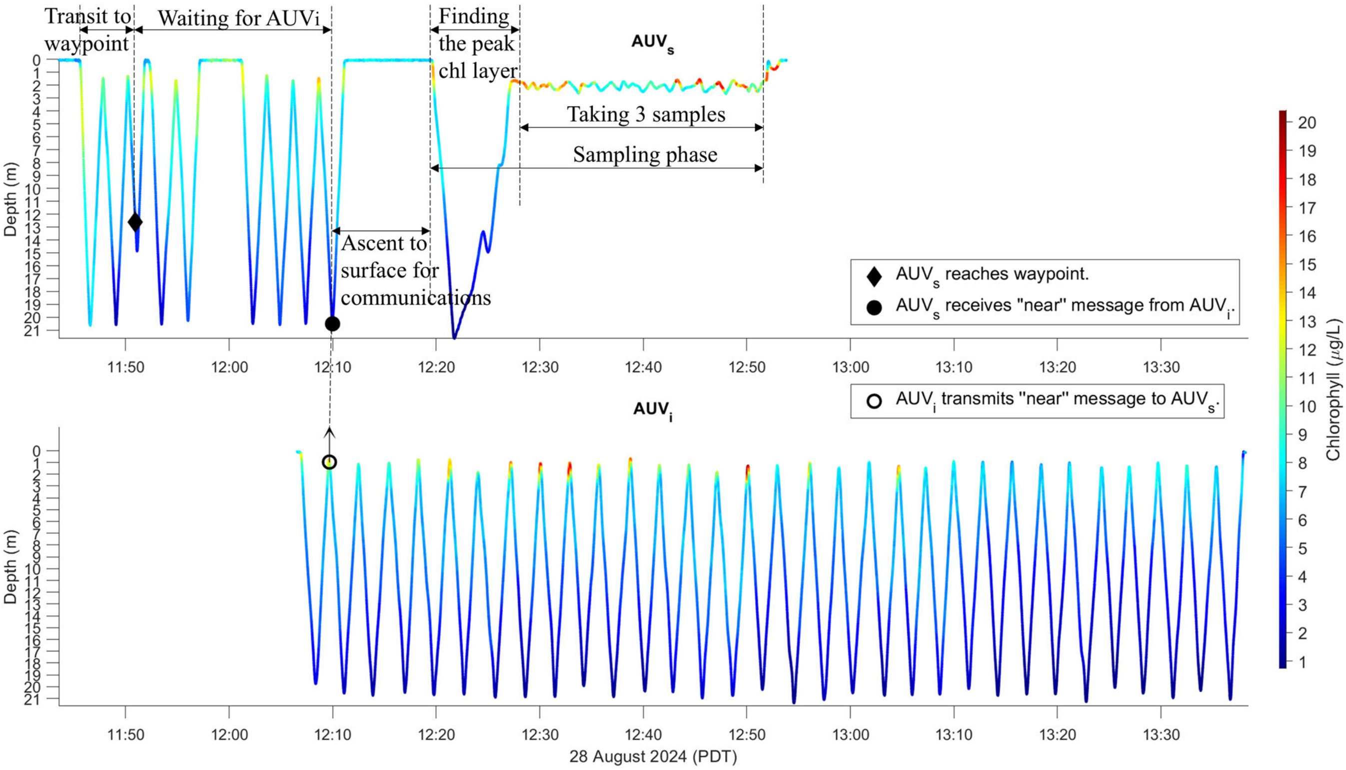

FIGURE 5 | Time series of AUV_s and AUV_i's depths (upper and lower panels, respectively; both color coded by the chlorophyll level) in the August 28 experiment. The sequential phases of AUV_s's mission and both vehicles' message transmission and reception events are marked and annotated. [Color figure can be viewed at wileyonlinelibrary.com]

chlorophyll level) are shown in Figure 5 which give the chronological order of AUV_s's mission phases and both vehicles' message transmission and reception events. The oblique and plan views of both vehicles' trajectories are shown in Figure 6 in which the vehicles' dead-reckoned locations during submergence have been corrected using the GPS fixes when on the sea surface.

At 11:43, AUV_s started the mission by flying westward to the waypoint on a yo-yo trajectory between 2-m and 20-m depths. At 11:51, the vehicle reached the waypoint and spiraled up and down (at a 30 m radius) at this location waiting for AUV_i's arrival. At 12:06, AUV_i started the mission by yo-yoing (also between 2-m and 20-m depths) northward to the waypoint. Due to the short initial distance between the two vehicles, AUV_i's DAT swiftly detected AUV_s to start acoustic tracking. At 12:10, AUV_i's DAT-measured range to AUV_s fell below the 100-m threshold ($thresh_{dist}$), so it acoustically transmitted a "near" message to AUV_s. On receiving the "near" message from AUV_i, AUV_s exited the wait-for-AUV_i phase and ascended to the sea surface to get GPS fixes and transmit vehicle data to shore via the Iridium satellite before starting the sampling phase.

At 12:19, AUV_s dove to find the peak chlorophyll layer. On the descent to 20-m depth ($Dep_{DeepBoundChl}$), the vehicle detected the chlorophyll peak at 2.1 m. On the ensuing ascent, the vehicle stopped ascending at the 2.1-m depth and circled (at a radius of about 20 m) at that depth to acquire three bags of water samples. Before taking the first sample, a 5-min lockout time allowed the vehicle's depth overshoot to damp down. Acquisition of each sample took about 4 min. The interval between the completion of one sample and the start of the next sample was set to 1 min.

At 12:51, AUV_s completed taking three samples. At this point, the vehicle's depth was 1.6 m, shallower than the 2 m setting of

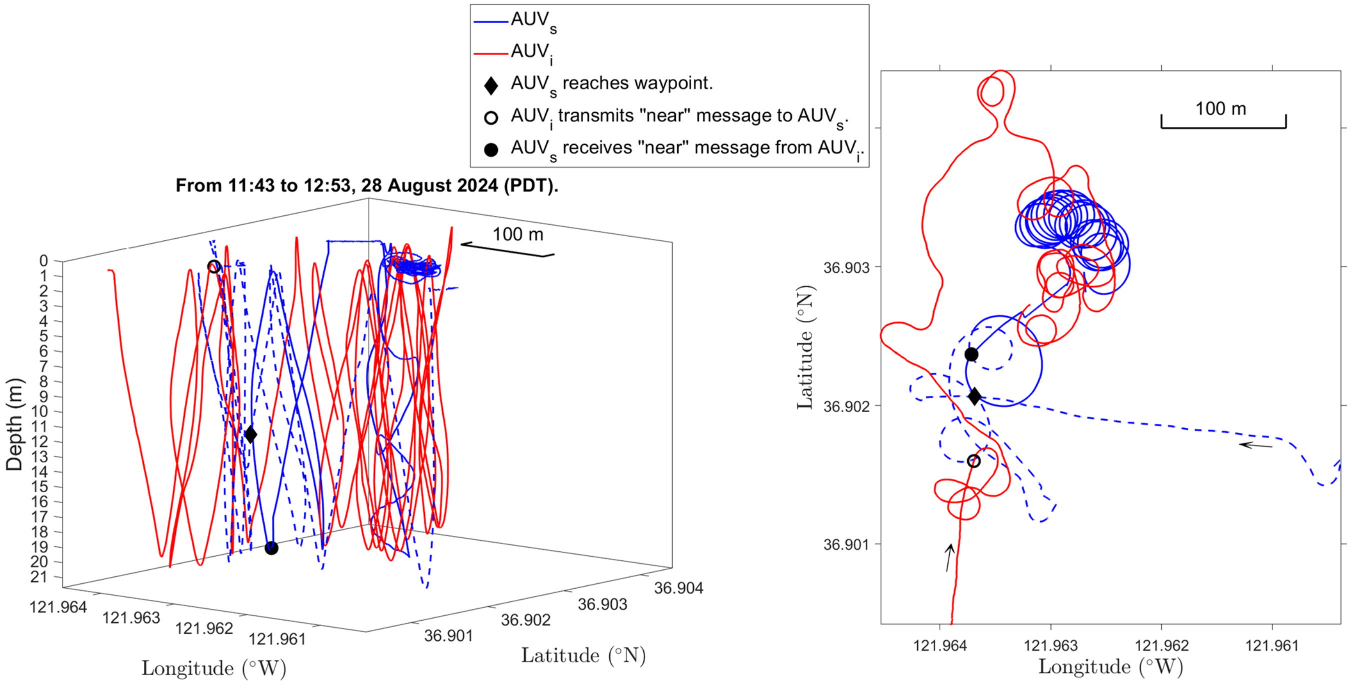

FIGURE 6 | Left panel: oblique view of AUV_s and AUV_i's trajectories in the August 28 experiment. Right panel: plan view. The locations where AUV_s reached the waypoint and the two vehicles transmitted and received the acoustic messages are marked using the same symbols as in Figure 5. The portion of AUV_s's trajectory before AUV_i's mission-start is plotted on the dashed line. [Color figure can be viewed at wileyonlinelibrary.com]

Dep_{minDAT}. Consequently, AUV_s did not transmit the "terminateMission" message to AUV_i, but just terminated its own sampling mission and ascended to the surface. After the experiments, we revised the algorithm to ensure the message gets transmitted at a depth deeper than Dep_{minDAT} and allow sufficient time for the other vehicle to receive the message (see Section 5).

At 13:38, when AUV_i surfaced for the periodic (every 1.5 h) surface communications, it received a "stop" command sent by the LRAUV operator via the Iridium satellite to terminate the mission. Because AUV_s's sampling mission already ended at 12:51, the last 47 min (from 12:51 to 13:38) of AUV_i's imaging mission was not useful. This instance of the absence of the "terminateMission" message highlighted its importance for preventing waste of time.

4.2 | Experiment on August 29, 2024

The sampling waypoint was at 36.75°N, 121.88°W. The time series of AUV_s and AUV_i's depths (color coded by chlorophyll level) are shown in Figure 7 which give the chronological order of AUV_s's mission phases and both vehicles' message transmission and reception events. The oblique and plan views of both vehicles' trajectories are shown in Figure 8 in which the vehicles' dead-reckoned locations during submergence have been corrected using the GPS fixes when on the sea surface.

At 15:06, AUV_i started the mission by yo-yoing (between 2-m and 20-m depths) southwestward to the waypoint. At 15:20, AUV_s started the mission by yo-yoing (also between 2-m and 20-m depths) south-southwestward to the waypoint. After AUV_s's submergence, AUV_i's DAT swiftly detected AUV_s to start acoustic tracking. At 15:24, AUV_i's DAT-measured range to AUV_s fell below the 100-m threshold, so it transmitted a "near" message to AUV_s. When receiving this message, AUV_s had not yet reached the waypoint, so it continued the transit toward the waypoint. When reaching the waypoint at 15:30, AUV_s bypassed the wait-for-AUV_i phase because the reception of the "near" message from AUV_i at 15:24 had informed AUV_s of AUV_i's closeness. AUV_s ascended to the sea surface to get GPS fixes and transmit vehicle data to shore via the Iridium satellite before starting the sampling phase.

At 15:38, AUV_s dove to find the peak chlorophyll layer. On the descent to 20-m depth, the vehicle detected the chlorophyll peak at 4.4 m. On the ensuing ascent, the vehicle stopped ascending at the 4.4-m depth and circled (at a radius of about 20 m) at that depth to acquire three water samples in the same sequence as in the August 28 experiment. Note that there was an eastward current of 0.13 m/s, estimated from the differences between the vehicle's dead-reckoned and GPS-fix locations.

At 16:12, AUV_s completed taking three samples. It acoustically transmitted a "terminateMission" message to AUV_i, and then terminated its own sampling mission and ascended to the surface. AUV_i received the message to terminate the imaging mission and also ascended to the surface. Thanks to the "terminateMission" message, AUV_i promptly ended its mission without wasting any time.

5 | Conclusion and Discussion

We developed a method of collaborative sampling and imaging by two LRAUVs (equipped with a water sampler and a microscopy system respectively) using inter-vehicle acoustic

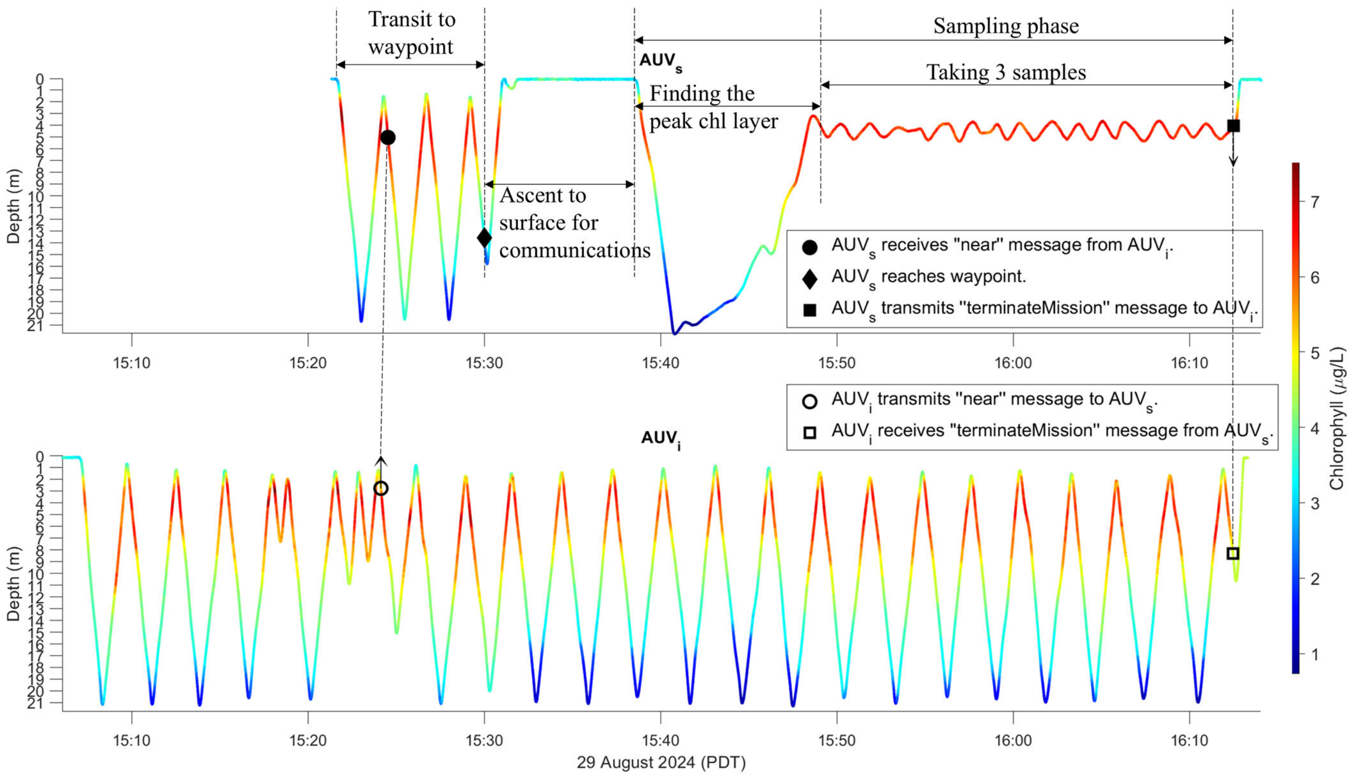

FIGURE 7 | Time series of AUV_s and AUV_i's depths (upper and lower panels, respectively; both color coded by the chlorophyll level) in the August 29 experiment. The sequential phases of AUV_s's mission and both vehicles' message transmission and reception events are marked and annotated. [Color figure can be viewed at wileyonlinelibrary.com]

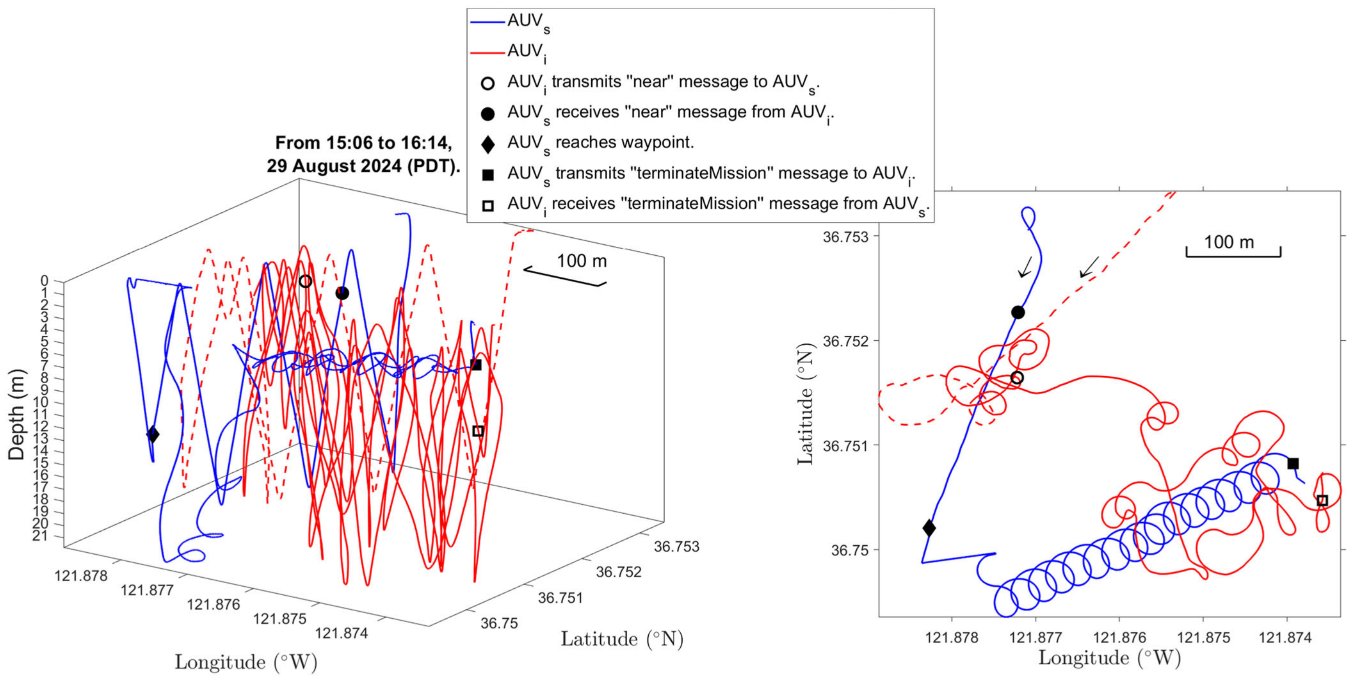

FIGURE 8 | Left panel: oblique view of AUV_s and AUV_i's trajectories in the August 29 experiment. Right panel: plan view. The locations where AUV_s reached the waypoint and the two vehicles transmitted and received the acoustic messages are marked using the same symbols as in Figure 7. The portion of AUV_i's trajectory before AUV_s's mission-start is plotted on the dashed line. [Color figure can be viewed at wileyonlinelibrary.com]

tracking and messaging. This method was used in studies of taxonomic composition of phytoplankton communities in Monterey Bay in August 2024. DNA analysis of the water samples is under way.

In the August 28 experiment, when AUV_s completed sampling, its depth was shallower than Dep_{minDAT}. Consequently, AUV_s did not transmit the "terminateMission" message to AUV_i. In other trials, we noticed another issue. AUV_s's transmission of the "terminateMission" message occurred right before the end of its own mission. Not enough time was left for AUV_s to retransmit the message if not immediately receiving acknowledgment from AUV_i.

After the experiments, we improved the algorithm: after the sampling task is completed, the sampling vehicle circles at a depth (e.g., 5 m) deeper than Dep_{minDAT} for a certain duration (e.g., 1 min) (the depth and the duration are both programmable parameters) to give sufficient time for the sampling vehicle to transmit (and retransmit) the "terminateMission" message and for the imaging vehicle to receive the message. Then the sampling vehicle ends its own mission.

Acoustic messages can contain not only navigation status (e.g., "near") and operational instruction (e.g., "terminateMission") but also a variety of information extracted from LRAUV measurements (e.g., real-time toxin levels reported by an LRAUV-borne 3G-ESP (Ussler III et al. 2024). By exchanging such messages, the collaborative LRAUVs can promptly adapt behaviors and accomplish tasks efficiently. We will extend the collaboration method to more vehicles (e.g., three vehicles carrying out sampling, imaging, and bioacoustic monitoring, respectively) exchanging acoustic messages containing operational and data information.

In addition to underwater vehicles, a Wave Glider on the sea surface can use its own acoustic modem to receive messages from the submerged LRAUVs and then relay these messages to shore via cellular or satellite communications to provide real-time situational awareness for the onshore operator. In the reverse direction, the onshore operator can send commands to the LRAUVs via the Wave Glider when intervention is necessary. We will continue to develop message-based multi-vehicle collaboration methods to advance targeted sampling of oceanographic features (Zhang et al. 2019; Scholin et al. 2025).

Acknowledgments

This study was supported by the David and Lucile Packard Foundation. We thank Jon Erickson, Aaron Schnittger, Denis Klimov, and Irene Hu for their contributions to the development and tests of the "Planktivore" microscopy system. We thank Larry Bird for the development of the "Sipper" water sampler. We are thankful to Christopher Wahl and Evan Mattiasen for helping with the LRAUV operation, Carlos Rueda for developing and supporting the LRAUV operation portal, and Mariah Salisbury for the help with Figure 1. The authors appreciate the helpful comments from the anonymous reviewers.

Data Availability Statement

The data that support the findings of this study are available from the corresponding author upon reasonable request.

References

Bellingham, J. G., and T. R. Consi. 1990. "State Configured Layered Control." In *Proceedings of IARP 1st Workshop on Mobile Robots for Subsea Environments*, 75–80.

Bellingham, J. G., Y. Zhang, J. E. Kerwin, et al. 2010. "Efficient Propulsion for the Tethys Long-Range Autonomous Underwater Vehicle." In *Proceedings of IEEE AUV'2010*, 1–6.

Biggs, B., D. J. Stilwell, H. Yetkin, and J. McMahon. 2024. "Efficient Feature Mapping Using a Collaborative Team of AUVs." In *Proceedings of IEEE/RSJ International Conference on Intelligent Robots and Systems*, 1–8.

Chavez, F. P., J. T. Pennington, R. P. Michisaki, et al. 2017. "Climate Variability and Change: Response of a Coastal Ocean Ecosystem." *Oceanography* 30, no. 4: 128–143.

Falkowski, P., and D. A. Kiefer. 1985. "Chlorophyll a Fluorescence in Phytoplankton: Relationship to Photosynthesis and Biomass." *Journal of Plankton Research* 7, no. 5: 715–731.

Fischell, E. M., N. R. Rypkema, and H. Schmidt. 2019. "Relative Autonomy and Navigation for Command and Control of Low-Cost Autonomous Underwater Vehicles." *IEEE Robotics and Automation Letters* 4, no. 2: 1800–1806.

Hine, R., S. Willcox, G. Hine, and T. Richardson. 2009. "The Wave Glider: A Wave-Powered Autonomous Marine Vehicle." In *Proceedings of MTS/IEEE Oceans'09*, 1–6.

Hobson, B., J. G. Bellingham, B. Kieft, R. McEwen, M. Godin, and Y. Zhang. 2012. "Tethys-Class Long Range AUVs - Extending the Endurance of Propeller-Driven Cruising AUVs From Days to Weeks." In *Proceedings of IEEE AUV'2012* 1–8.

Leonard, N. E., D. A. Paley, R. E. Davis, D. M. Fratantoni, F. Lekien, and F. Zhang. 2010. "Coordinated Control of an Underwater Glider Fleet in an Adaptive Ocean Sampling Field Experiment in Monterey Bay." *Journal of Field Robotics* 27, no. 6: 718–740.

Lin, Y., J. Hsiung, R. Piersall, C. White, C. G. Lowe, and C. M. Clark. 2017. "A Multi-Autonomous Underwater Vehicle System for Autonomous Tracking of Marine Life." *Journal of Field Robotics* 34, no. 4: 757–774.

Manley, J., and S. Willcox. 2010. "The Wave Glider: A Persistent Platform for Ocean Science." In *Proceedings of IEEE Oceans'10* 1–5.

Messié, M., I. Shulman, S. Martini, and S. H. D. Haddock. 2019. "Using Fluorescence and Bioluminescence Sensors to Characterize Auto- and Heterotrophic Plankton Communities." *Progress in Oceanography* 171: 76–92. https://doi.org/10.1016/j.pocean.2018.12.010.

O'Brien, M., J. Williams, S. Chen, A. Pitt, R. Arkin, and N. Kottege. 2023. "Dynamic Task Allocation Approaches for Coordinated Exploration of Subterranean Environments." *Autonomous Robots* 47: 1559–1577.

Orenstein, E. C., D. Ratelle, C. Briseño-Avena, et al. 2020. "The Scripps Plankton Camera System: A Framework and Platform for In Situ Microscopy." *Limnology and Oceanography: Methods* 18: 681–695.

Paley, D., F. Zhang, and N. E. Leonard. 2008. "Cooperative Control for Ocean Sampling: The Glider Coodinated Control System." *IEEE Transactions on Control Systems Technology* 16, no. 4: 735–744.

Paull, L., G. Huang, M. Seto, and J. J. Leonard. 2015. " Communication Constrained Multi-AUV Cooperative SLAM." In Proceedings of IEEE International Conference on Robotics and Automation, 509–516.

Petillo, S., and H. Schmidt. 2014. "Exploiting Adaptive and Collaborative AUV Autonomy for Detection and Characterization of Internal Waves." *IEEE Journal of Oceanic Engineering* 39, no. 1: 150–164.

Rypkema, N. R., H. Schmidt, and E. M. Fischell. 2022. "Synchronous-Clock Range-Angle Relative Acoustic Navigation: A Unified Approach to Multi-AUV Localization, Command, Control, and Coordination." *Field Robotics* 2: 774–806.

Scholin, C. 2025. "Oceanography in the Age of Intelligent Robots and a Changing Climate." *Oceanography* 38, no. 3. https://doi.org/10.5670/oceanog.2025.e310.

Scholin, C., J. Birch, S. Jensen, et al. 2017. "The Quest to Develop Ecogenomic Sensors: A 25-year History of the Environmental Sample Processor (ESP) as a Case Study." *Oceanography* 30, no. 4: 100–113.

Skorobogatov, G., C. Barrado, and E. Salamí. 2020. "Multiple UAV Systems: A Survey." *Unmanned Systems* 8, no. 2: 149–169.

Stanway, M. J., B. Kieft, T. Hoover, B. Hobson, A. Hamilton, and J. Bellingham. 2014. "Acoustic Tracking and Homing With a Long-Range AUV." In *Proceedings of MTS/IEEE Oceans'14*, 1–7.

Ussler, W., III, G. J. Doucette, C. M. Preston, et al. 2024. "Underway Measurement of Cyanobacterial Microcystins Using a Surface Plasmon Resonance Sensor on An Autonomous Underwater Vehicle." *Limnology and Oceanography: Methods* 22: 681–699.

Yilmaz, N. K., C. Evangelinos, P. F. J. Lermusiaux, and N. M. Patrikalakis. 2008. "Path Planning of Autonomous Underwater Vehicles for Adaptive Sampling Using Mixed Integer Linear Programming." *IEEE Journal of Oceanic Engineering* 33, no. 4: 522–537.

Zhang, Y., B. Kieft, B. Hobson, et al. 2020. "Autonomous Tracking and Sampling of the Deep Chlorophyll Maximum Layer in an Open-Ocean Eddy by a Long Range Autonomous Underwater Vehicle." *IEEE Journal of Oceanic Engineering* 45, no. 4: 1308–1321.

Zhang, Y., B. Kieft, B. W. Hobson, et al. 2024. "Coordinated and Collaborative Sampling by Two Long-Range Autonomous Underwater Vehicles." *IEEE Journal of Oceanic Engineering* 49, no. 4: 1–12.

Zhang, Y., J. Ryan, B. Hobson, et al. 2021. "A System of Coordinated Autonomous Robots for Lagrangian Studies of Microbes in the Oceanic Deep Chlorophyll Maximum." *Science Robotics* 6: eabb9138, 1–12.

Zhang, Y., J. P. Ryan, B. Kieft, et al. 2019. "Targeted Sampling by Autonomous Underwater Vehicles." *Frontiers in Marine Science* 6: Article 415, 1–12.

Supporting Information

Additional supporting information can be found online in the Supporting Information section.
Supplementary Information